

ac conductivity of tungsten phosphate glasses

Abhai Mansingh, R. P. Tandon,* and J. K. Vaid

Department of Physics and Astrophysics, University of Delhi, Delhi-110 007, India

(Received 18 June 1979)

The electrical conductivity in tungsten phosphate glasses of three different compositions (67 mole% of WO_3 -33 mole% P_2O_5 , 70 mole% WO_3 -30 mole% P_2O_5 , and 81 mole% WO_3 -19 mole% P_2O_5) has been measured in the frequency range 100 Hz to 3.60 GHz and in the temperature range 77-500°K. The measured ac conductivity at low temperature is almost independent of temperature but shows strong dependence on frequency according to the relation $\sigma(\omega) = A\omega^s$ where the exponent s has been observed to be less than unity. At higher temperatures the frequency dependence becomes weak at low frequencies and remains strong at higher frequencies. The weak frequency dependence is due to the contribution of dc conductivity to the measured ac conductivity. A clear Debye-type dielectric relaxation loss peak is observed by taking out the contribution of dc conductivity, but the frequency dependence of conductivity remains less than quadratic at low frequencies indicating some distribution of relaxation times. This behavior is confirmed by the variation of dielectric constant with frequency and temperature. The temperature and frequency dependence of ac conductivity can be adequately explained in WO_3 - P_2O_5 systems by considering the contributions from two mechanisms, one giving an almost linear dependence of conductivity on frequency, and the other having a narrower distribution of relaxation times giving rise to clear but broad dielectric loss peaks.

I. INTRODUCTION

The frequency dependence of electrical conductivity of amorphous solids has been the subject of detailed theoretical and experimental investigations.¹⁻⁴ ac conductivity due to hopping conduction increases with increasing frequency ω and is proportional to ω^s , where s is a parameter. Such a frequency dependence, which has been attributed to a wide distribution of relaxation times due to distribution of jump distances⁵ and barrier heights⁶ has been observed in a wide variety of low mobility materials.⁷ Most of the workers agree that at low frequencies (up to 10^5 Hz) and temperatures the exponent s has a value less than unity, but there is controversy as to whether s attains a value of two at high frequencies or remains close to unity even up to frequencies of the order of 10^{10} Hz. Owen and Robertson⁸ and Kitao *et al.*⁹ have reported a quadratic frequency dependence in the high-frequency region (above 10^5 Hz) in chalcogenide glasses. Linsley *et al.*¹⁰ have noted a similar frequency dependence in vanadate glasses. Lakatos and Abkowitz¹¹ have shown that a quadratic frequency dependence at high frequencies may be an outcome of the resistance of the electrodes. A value of s less than unity up to microwave frequencies has been reported by Bishop *et al.*¹² and Lakatos and Abkowitz for chalcogenide glasses and Sayer *et al.*¹³ for vanadate glasses. The variation of exponent s with temperature is also not clearly understood. Some models^{6,14-16} have been proposed to explain the temperature

dependence of ac conductivity and the variation of the exponent s with temperature. However, these models are applicable only within a limited numerical value of s close to but less than unity and can explain the behavior of ac conductivity only within a limited range of temperature. Apart from the controversy of the variation of s with temperature and frequency in the region where ac conductivity is substantially higher than dc conductivity, there is some uncertainty whether a Debye-type dielectric loss peak exists in the region where ac conductivity approaches dc conductivity.¹⁷ In this region the electrode polarization and sample inhomogeneity greatly influence the dielectric values, hence careful measurements are required to investigate this region.

The ac conductivity of several systems in chalcogenide glasses has been reported^{8,9,11,12} while in transition-metal ion phosphate glasses, the detailed studies have been made only in vanadium glasses.^{10,13,17,18} In this paper we report the results of our measurements on three different compositions of tungsten glasses (WO_3 - P_2O_5) in the temperature range 77-500 °K. It has been observed that Debye-type relaxation loss peaks with a distribution of relaxation times exist in the temperature region where ac conductivity approaches dc conductivity. However, almost linear frequency-dependent conductivity in the region where ac conductivity is substantially higher than dc conductivity suggests that two relaxation mechanisms have to be considered to explain the ac conductivity.

TABLE I. The physical parameters of the transition-metal-oxide phosphate glasses on which the present measurements have been made.

Glass system		No. of TMI (<i>N</i>) $\times 10^{22} \text{ cm}^{-3}$	TMI spacing (\AA)	Reduced TMI ratio	Density gm/cm^3
Starting composition	Analyzed composition				
67% WO_3 - 33% P_2O_5	65% WO_3 - 35% P_2O_5	0.87	4.86	0.007	4.4
70% WO_3 - 30% P_2O_5	71% WO_3 - 29% P_2O_5	0.94	4.74	0.006	4.6
81% WO_3 - 19% P_2O_5	78% WO_3 - 22% P_2O_5	1.13	4.46	0.004	5.0

II. EXPERIMENTAL

Three glasses in the WO_3 - P_2O_5 systems with composition 67, 70, and 81 mole% WO_3 were prepared by melting the oxides (WO_3 : Kochlight 99.9% pure, P_2O_5 Pfizer 99.9% pure) in a platinum crucible for two hours at 1200 °C in air atmosphere. The glasses were then formed by pouring the melt onto a copper plate held at room temperature. The absence of crystals was verified by x-ray analysis. The final composition was determined by estimating WO_3 by chemical analysis. The total number of tungsten sites was estimated from the analyzed composition and the reduced W^{5+} ions were determined from the EPR studies. The EPR spectra of the samples were taken on a varian E-12 spectrograph. The shape of the spectra was similar to that reported by Lynch *et al.*¹⁹ and Sayer and Lynch²⁰ for other oxide glasses and the total number of spins was found to be independent of temperature in the range 77 to 300 °K. The physical parameters of the samples studies are reported in Table I.

The samples of convenient shape and size (typically $1 \times 0.7 \times 0.2 \text{ cm}$) were cut and polished which were then annealed for two hours at 200 °C to remove any mechanical stress and a further annealing of one hour at this temperature was needed after vacuum deposition of the gold electrodes on the sample to get the Ohmic contacts. The Ohmic contacts were checked by studying I-V characteristics. It was seen that normally a good Ohmic contact could be obtained only on proper annealing of the sample.

The measurements were made in the temperature range 77–500 °K on a GR-716 CS Schering bridge. The details of measuring technique have been reported elsewhere.²¹ The values of dielectric constant and conductivity could be reproduced within 3% and 5%, respectively, in different runs. To check the variation of conductivity with frequency at higher frequencies, measurements were made at room temperature by employing a Wayne

Kerr bridge (B601 radio frequency bridge) in the range 15 KHz to 5 KHz and *Q* meter (Boonton Radio 190A) in the range 100 KHz to 100 MHz. The agreement between the measured values in overlapping ranges of Schering bridge and Wayne-Kerr bridge was within 4% while the values from *Q* meter showed a variation of 15%–20% in the overlapping range with Wayne-Kerr bridge. A cavity perturbation technique²² was employed at 3.6 GHz.

III. RESULTS

The measured conductivity of an 81% WO_3 -19% P_2O_5 glass at different temperatures and five fixed frequencies (radio and microwave frequencies) is shown in Fig. 1. The figure looks similar to that reported for vanadium phosphate glasses.²³ The overall behavior of the other samples of tungsten glasses of different compositions was similar except for the difference in the numerical values and the temperature at which the measured ac conductivity becomes equal to dc conductivity.

It can be seen from the Fig. 1 that the tempera-

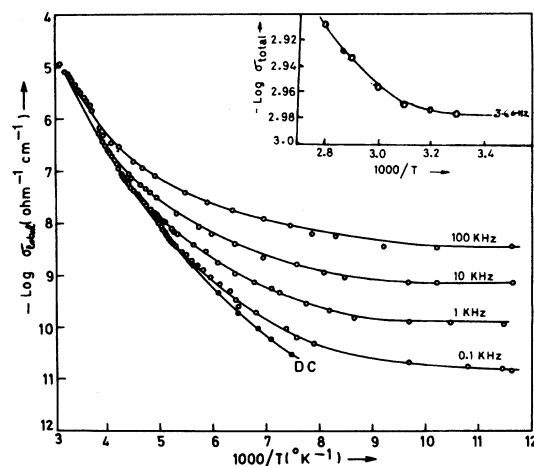


FIG. 1. Total measured conductivity σ_{tot} plotted vs $1000/T$ for fixed frequencies of measurement for 81/19 tungsten phosphate glass. The insert shows the microwave conductivity on an enlarged scale.

TABLE II. The measured ac conductivity at 1 KHz and slope s at different temperatures, and the calculated values of parameters B from Eq. (8). The density of states $N(E_F)$ calculated from Eq. (9) assuming $\nu_0 = 10^{13}$ Hz and $\alpha = 0.3$ and 1 \AA are also included in the table.

Glass system	Temperature T ($^{\circ}\text{K}$)	at		B in esu.	$N(E_F)$ taking $\alpha = 0.3 \text{ \AA}$	$N(E_F)$ taking $\alpha = 1 \text{ \AA}$
		1 KHz cm^{-1}	Slope s		$\times 10^{22} \text{ cm}^{-3} \text{ eV}^{-1}$	$\times 10^{21} \text{ cm}^{-3} \text{ eV}^{-1}$
67% WO_3	95	0.89×10^{-10}	0.78	9.19×10^{-4}	2.99	1.47
	125	1.33×10^{-10}	0.74	...	3.19	1.57
70% WO_3	95	1.0×10^{-10}	0.76	1.34×10^{-3}	3.17	1.56
	125	1.99×10^{-10}	0.74	...	3.90	1.92
81% WO_3	95	1.41×10^{-10}	0.80	1.22×10^{-3}	3.77	1.85
	125	2.28×10^{-10}	0.73	...	4.17	2.06

ture dependence of conductivity starts at higher temperature for higher frequencies. The conductivity at 3.6 GHz shows little variation with temperature in the range 300–320 $^{\circ}\text{K}$. Such a region for 100 KHz is observed at much lower temperature (95–130 $^{\circ}\text{K}$).

Kabashima *et al.*²⁴ have tried to improve upon the Pollak and Geballe⁵ expression to explain the strong temperature dependence of ac conductivity by taking into account the disorder energy term. However, the expression suggested by Kabashima *et al.* predicts a rapid increase of conductivity for all the frequencies at the same temperature, whereas the present studies (Fig. 1) show that the strong temperature dependence starts at higher temperature for higher frequencies.

At low temperatures the ac conductivity $\sigma(\omega)$ is proportional to ω^s , where the slope s is less than unity. There is not much change in slope s with temperature below 95 $^{\circ}\text{K}$, $\sigma(\omega)$ shows a linear dependence on temperature at all frequencies below 95 $^{\circ}\text{K}$. In this low-temperature region the conductivity can be given by³

$$\sigma(\omega) = \frac{\pi^3}{96} e^2 k T [N(E_F)]^2 \alpha^5 \omega \left[\ln \left(\frac{\nu_0}{\omega} \right) \right]^4, \quad (1)$$

where $N(E_F)$ is the number of sites per unit energy for unit volume, α is the radius of the localized electron wave function, and ν_0 is the characteristic phonon frequency. The measured conductivity at low temperatures can be used to estimate the value of $N(E_F)$, but the numerical magnitude of $N(E_F)$ will depend strongly on the value of α and is rather insensitive to the value ν_0 which may be taken as $10^{13}/\text{sec}$. A value of α in the range 1 to 0.3 \AA has been suggested for vanadium phosphate glasses. The value of $N(E_F)$ calculated by taking α equal to 1 and 0.3 \AA are reported in Table II. A value of 0.3 \AA leads to the value of $N(E_F)$ as $10^{22} \text{ cm}^{-3} \text{ eV}^{-1}$. Such a large density of states would suggest extended rather

than localized states. Even the value of unity for α gives $N(E_F)$ a value of the order 10^{21} , hence a higher value for the radius of localized electron wave function seems more appropriate which will give $N(E_F)$ a value of the order of 10^{19} – 10^{20} . The value of unity or even two for α will satisfy the condition of uncorrelated hops,

$$\left[\frac{4}{3} \pi N(E_F) k T \right]^{1/3} > \alpha \ln \frac{\nu_0}{\omega} \quad (2)$$

for which Eq. (1) is valid.

Above 95 $^{\circ}\text{K}$ a rapid decrease of slope with increasing temperature is evident from Fig. 2. It can be noticed in Figs. 1 and 2 that the decrease of s with increasing temperature is an outcome of larger increase of conductivity with temperature at low frequencies as compared to that at higher frequencies.

Pike⁶ has attempted to explain the temperature dependence of conductivity and the exponent s . He suggests the following expression:

$$1 - s = 6kT/W, \quad (3)$$

where W is the activation energy and k is the

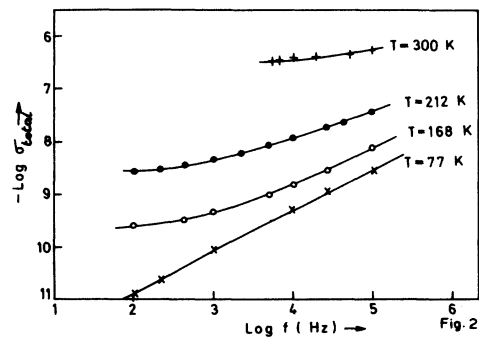


FIG. 2. Measured conductivity of 67/33 tungsten phosphate glass at four fixed temperatures as a function of frequency.

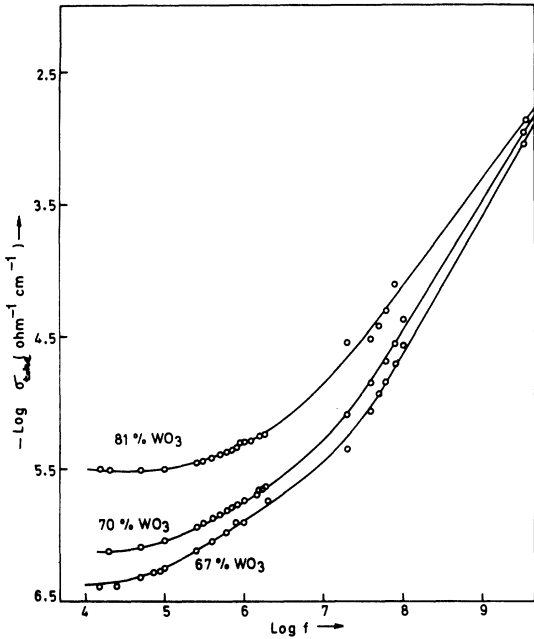


FIG. 3. Total measured conductivity plotted as a function of frequency at room temperature for the three glass systems.

Boltzmann constant. Springett and Elliott have also suggested a similar temperature dependence of s . If we take value of s at 100 °K as 0.8 the value at 300 °K would come out to be 0.4. The experimental values of slope evident from Fig. 2 do not suggest

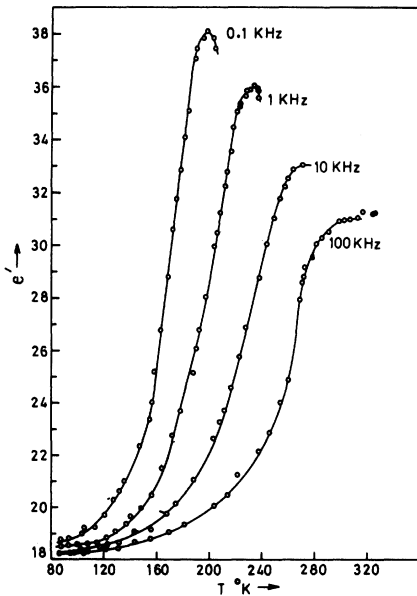


FIG. 4. Temperature dependence of dielectric constant measured at different frequencies for 81/19 tungsten phosphate glass.

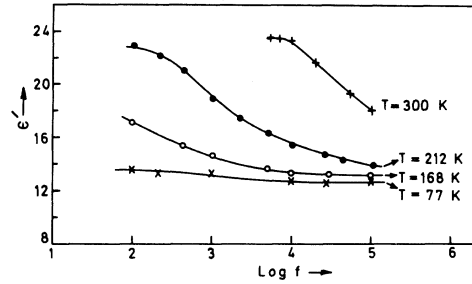


FIG. 5. Measured dielectric constant of a 67/33 tungsten phosphate glass at four fixed temperatures as a function of frequencies.

such a temperature dependence. Apart from this, the value of slope depends on measuring frequency and temperature. It may be noted in Fig. 3 that the slope at high frequencies above 5×10^6 Hz at room temperature is not lower than that observed at low frequencies and is close to unity. Thus the models proposed to explain the temperature dependence of ac conductivity and slope s cannot explain the data of $WO_3-P_2O_5$ glass.

The variation of dielectric constant ϵ' as a function of temperature at four fixed frequencies is shown in Fig. 4. The curves look very similar to that reported for $V_2O_5-P_2O_5$ glass.^{2,3} The dielectric behavior of other samples was similar to that reported in Fig. 4 except for the numerical difference and the temperature at which a peak in the measured dielectric constant is obtained at a given frequency. The variation of dielectric constant as a function of frequency and temperature is given in Fig. 5. There is very little variation of the dielectric constant with frequency at 77 °K, while at higher temperatures the dielectric constant shows a large dispersion. It may be noted from Figs. 2 and 5 that the variation of dielectric constant with frequency is very small in the region where the

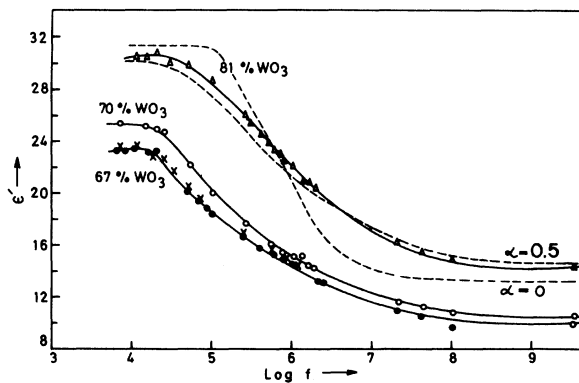


FIG. 6. Measured dielectric constant as a function of frequency at room temperature for the three glasses.

conductivity shows a linear frequency dependence, while the variation is large in the region where conductivity shows weak frequency dependence. The measured values of the dielectric constant for three samples at room temperature up to a frequency of 3.60 GHz are shown in Fig. 6.

IV. DISCUSSIONS

A. Region I: Where ac conductivity approaches dc conductivity

The measurements as a function of temperature (Fig. 1) show that the temperature at which the dc conductivity becomes equal to the total measured ac conductivity σ_{tot} for a given frequency increases with increasing frequency. The dc conductivity shows an exponential dependence on temperature while ac conductivity shows only a linear dependence on temperature. Hence at some temperature measured conductivity σ_{tot} for a given frequency and dc conductivity σ_{dc} will appear equal because the dc conductivity may be very much higher than ac $\sigma(\omega)$, and so the measured values within the accuracy of measurement will appear equal to dc.²³ Thus the dielectric loss peak derived from the following relation:

$$\omega \delta_0 \epsilon'' = \sigma_{\text{tot}} - \sigma_{\text{dc}} = \sigma(\omega) \quad (4)$$

may be real or may be due to the different temperature dependence of ac and dc conductivity.

The dielectric constant for Debye-type dispersion is expressed by²⁵

$$\epsilon' - \epsilon_{\infty} = \frac{\epsilon_0 - \epsilon_{\infty}}{1 + \omega^2 \tau^2}, \quad (5)$$

where ϵ' is the measured dielectric constant at frequency ω and ϵ_0 and ϵ_{∞} are the low- and high-frequency dielectric constants. τ is the relaxation frequency $f_0 = 1/2\pi\tau$. At low temperatures, $\omega\tau$ is expected to be very much greater than unity, and the measured ϵ' approaches ϵ_{∞} as shown in Fig. 4. A strong increase of dielectric constant with temperature will be shown in the temperature region where the measuring frequency approaches relaxation frequency. The temperature region where the strong temperature dependence is shown at a given frequency should increase with increasing frequency because f_0 is expected to increase with increasing temperature. The temperature-dependent dielectric constant shown in Fig. 4 is consistent with a Debye-type dispersion. At higher temperatures where $\omega\tau$ is very much smaller than unity, the measured dielectric constant will be equal to the static dielectric constant. A decrease in the measured values with temperature at a fixed frequency indicates that the static value has been reached, and the static dielectric constant decreases with increasing temperature. Figures

4, 5, and 6 are consistent with the Debye-type dispersion and suggest that the loss peaks [derived from Figs. 1 and 3 and Eq. (4)] are real. The existence of well-defined loss peaks has also been observed in silicate glasses^{26,27} and amorphous films of MoO_3 ²⁸ and WO_3 .²⁹ This behavior of transition-metal ion (TMI) phosphate glasses is different from that reported for chalcogenide glasses. In chalcogenide glasses very little (10%) dispersion is observed¹¹ between 100 Hz and 10 GHz or between room temperature and 77 °K at 100 Hz. However, strong dielectric dispersion is observed in the region where measured ac conductivity approaches dc conductivity, and very little dispersion is observed in the region where the ac conductivity is substantially higher than the dc conductivity. The dielectric constant in chalcogenide glasses has not been reported in the region where ac and dc conductivities are equal and so it can not be conclusively said that the behavior of TMI phosphate glasses is different from chalcogenide glasses. Recently Shimakawa *et al.*³⁰ have reported the dielectric relaxation loss peaks in doped and undoped As_2Se_3 glasses.

A Debye-type dispersion in the region where ac conductivity approached dc conductivity could be due to the following three reasons: (1) Maxwell-Wagner polarization due to the presence of inhomogeneities,³¹ (2) the electrode polarization due to surface barriers,³² and (3) true bulk effect.

The presence of crystalline WO_3 in the glassy matrix can be thought of as a possible source of inhomogeneity. However, there was no effect in the absolute value of conductivity and the positions of loss peaks on annealing the samples at 200 °C for four hours suggesting the absence of crystallites. Moreover, crystalline WO_3 gives phase transitions at about -40 and +17 °C where a drastic change in conductivity and the activation energy occurs.³³ The phase transitions due to small amount of crystalline WO_3 are not expected to be very sharp, but some discontinuity in the conductivity versus temperature plot should have been indicated. However, no such discontinuities are indicated in Fig. 1. Hence it may be concluded that the dielectric dispersion is not due to the presence of inhomogeneities.

The surface capacitance is expected to be independent of the thickness of the sample. If the low-frequency or the high-temperature dielectric constant values which are considerably higher than the microwave or low-temperature value are indicative of the surface barrier, then the static dielectric constant should decrease with a decrease in sample thickness provided the area is kept constant. Measurements were made at room temperature in the frequency region 10^4 to 10^6 Hz by

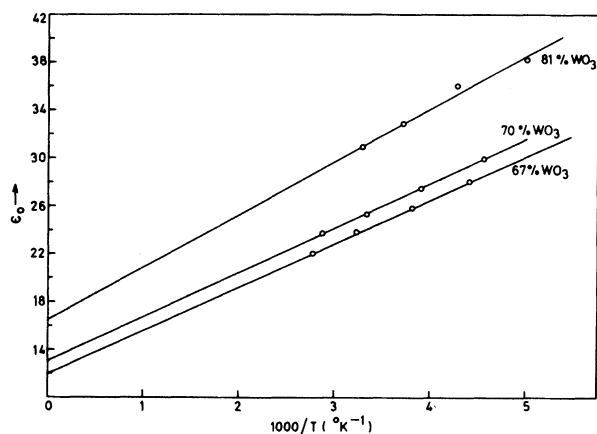


FIG. 7. Plot of static dielectric constant ϵ_0 against $1000/T$ for the three glasses.

changing the thickness of the sample from 2 to 1 mm while the area was kept constant. The results for one glass (67% $\text{WO}_3 - \text{P}_2\text{O}_5$) are shown in Fig. 6. It may be seen that the dielectric constant is independent of the thickness and the scatter is within the experimental accuracy. This suggests that the dielectric dispersion is not due to the surface barrier or electrode polarizations. The above discussions rule out the possibility of dielectric dispersion due to spurious effects and it appears to be a true bulk property. The variation of static dielectric constant ϵ_0 with temperature can be found from Fig. 4, because the value at the peak and after it represent ϵ_0 . A plot of ϵ_0 vs $1/T$ is shown in Fig. 7. The temperature variation is in accordance with following relation¹⁸:

$$\epsilon_0 - \epsilon_\infty = \frac{4\pi}{3} \frac{Ne^2\gamma^2}{kT} c(1-c), \quad (6)$$

where N is the number of sites per unit volume, c is the fraction of reduced sites, and γ is the average site spacing. The extrapolated values of infinite-frequency dielectric constant are close to the measured value at 3.6 GHz. The numerical

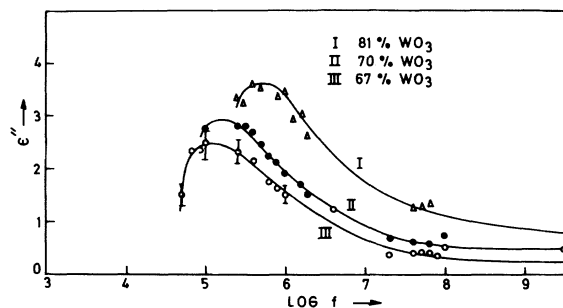


FIG. 8. Derived dielectric loss as a function of frequency at room temperature for the three glasses.

values of $\epsilon_0 - \epsilon_\infty$ calculated from the relation (6) are tabulated in Table III. It may be noted that the calculated values are about one-sixth of the measured values. This large error may be due to the uncertainty about the actual number of carriers contributing to the dielectric constant and taking the average site spacing as the distance between the charges of the dipole.²⁹

The dielectric loss values calculated from Eq. (4) using the measured values from Fig. 3 are shown in Fig. 8. A clear peak in ϵ'' is observed. However, the values of dielectric loss are derived from the measured conductivity in the region where the measured ac conductivity becomes close to dc conductivity; the errors in the measurements of conductivity give a large error in ϵ'' . To give an idea of the magnitude of the error, the estimated error for one sample is shown in Fig. 8. The uncertainty in relaxation frequency is of the order of 100%. The half-width of the plots of ϵ'' against the logarithm of frequency should be 1.40 decade for a Debye-type dispersion with a single relaxation time. However, the width of Fig. 8 appears to be of the order of 2 to 3 decades of frequency suggesting some distribution of relaxation times.

An estimate of the relaxation time can also be made from measured dielectric constant (Figs. 5

TABLE III. Measured values of activation energy W_H and dielectric constant for different composition tungsten phosphate glasses. The values calculated from Eq. (6) are also included in the table.

Glass system	dc activation energy W_H (eV) at 300°K	W_H (eV) from Fig. 10 at 300°K	Static dielectric constant ϵ_0	Measured ϵ' at 3.6 GHz	Measured ϵ_∞	$\epsilon_0 - \epsilon_\infty$ calculated
67% WO_3	0.33	0.36	24.0	12.0	12	3.31
70% WO_3	0.32	0.36	25.2	13.2	13	2.93
81% WO_3	0.30	0.32	31.0	16.4	16.4	2.08

and 6). It can be seen from Eq. (5) that the temperature at which $\epsilon' - \epsilon_\infty$ at a given frequency is equal to $(\epsilon_0 - \epsilon_\infty)/2$; then $\omega\tau = 1$ and the measuring frequency will be equal to the relaxation frequency. The estimation of relaxation frequency from the temperature variation of the dielectric constant at different frequencies is shown in Fig. 9, where the top solid line shows the static dielectric constant at different temperatures and the bottom dashed lines show the estimated values of ϵ_∞ considering extreme errors. The temperatures at which the measured dielectric constant at a given frequency is equal to $(\epsilon_0 - \epsilon_\infty)/2 + \epsilon_\infty$ are marked by crosses. If we assume a maximum error of about 20% in the estimated value of ϵ_∞ , then the corresponding errors in the temperature at which the measuring frequency becomes equal to the relaxation frequency will be $\pm 10^\circ\text{K}$ (indicated in Fig. 9). A plot of $\ln f_0$ against $1/T$ is shown in Fig. 10. The relaxation frequency f_0 can be represented by the relation $f = f'_0 e^{-W/kT}$, where f'_0 is a constant having dimensions of frequency and W is the activation energy. An error of $\pm 10^\circ\text{K}$ in temperature would correspond to a maximum error of about 100% in the relaxation frequency as is evident from Fig. 10. The activation energy calculated from Fig. 10 is reported in Table III.

The variation of dielectric constant with frequency shown in Fig. 6 indicates a Debye-type dispersion but does not correspond to a single relaxation time. The dielectric constant in the presence of symmetric distribution of relaxation times can be given by the Cole-Cole expression¹³

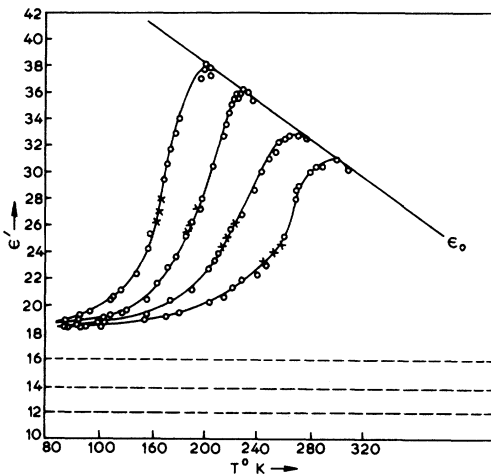


FIG. 9. Estimation of dielectric relaxation time from the measured temperature variation of dielectric constant at different frequencies. The top solid line corresponds to the static dielectric constant ϵ_0 . The bottom lines (dotted) correspond to $\epsilon_\infty = 12, 14, \text{ and } 16$.

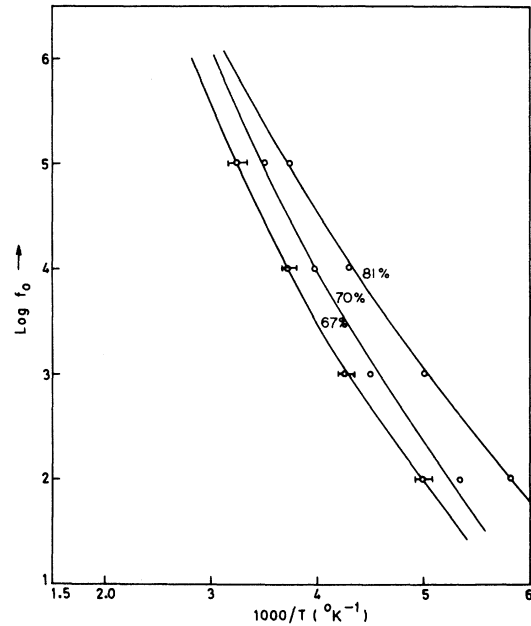


FIG. 10. Plot of relaxation frequency $f_0 = 1/2\pi\tau$ vs $1000/T$ for the three glasses.

$$\epsilon' - \epsilon_\infty = \frac{(\epsilon_0 - \epsilon_\infty) + (\omega\tau)^{1-\alpha}(\epsilon_0 - \epsilon_\infty) \sin(\alpha\pi/2)}{1 + 2(\omega\tau)^{1-\alpha} \sin(\alpha\pi/2) + (\alpha\tau)^2(1-\alpha)}, \quad (7)$$

where α is an empirical distribution parameter having the values between 0 and 1. A value of zero corresponds to a single relaxation time. The expected variation of dielectric constant with frequency for a single relaxation time corresponding to $\alpha = 0$ and for finite distribution of relaxation times ($\alpha = 0.5$) calculated from Eq. (7) by taking $\epsilon_0 = 30$, $\epsilon_\infty = 14$, and $f_0 = 10^5$ Hz, is shown in Fig. 6 for 81% $\text{WO}_3\text{-P}_2\text{O}_5$ glass. It may be noted in the figure that the experimental values closely correspond to Cole-Cole distribution parameter $\alpha = 0.5$.

The analysis of the dielectric constant data of WO_3 glasses indicates the existence of the dielectric dispersion due to the bulk effect in the region where ac conductivity approaches dc conductivity. The dielectric dispersion is not characterized by a single relaxation time, but a distribution of relaxation times is indicated.

B. Region II: Where ac conductivity is substantially higher than dc

The measured conductivity at different frequencies and dc conductivity level for a 67% $\text{WO}_3 - 33\%$ P_2O_5 glass is shown in Fig. 11. The conductivity up to about 1 MHz is quite close to the dc level, while beyond this frequency the measured ac conductivity is substantially higher than the dc con-

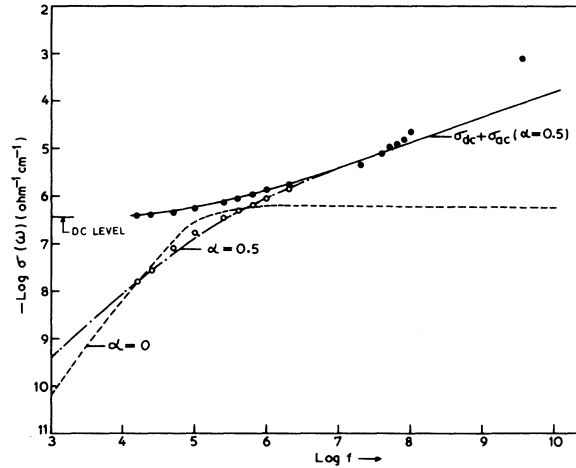


FIG. 11. The measured ac conductivity $\sigma(\omega)$ as a function of frequency for 67/33 WO_3 glass at room temperature as shown by filled circles. The calculated values from Eq. (8) are obtained by taking $\epsilon_0 = 23.2$, $\epsilon_\infty = 12$, $f_0 = 10^5$ Hz, shown by ----- for $\alpha = 0$ and - · - · - for $\alpha = 0.5$. The experimental points obtained by subtracting dc are shown by hollow circles.

ductivity. In the previous section it was shown that a well-defined dielectric loss peak with a distribution of relaxation times ($\alpha = 0.5$) exists in the region where ac conductivity approaches dc conductivity. It is worth seeing in the region where ac conductivity is substantially higher than dc conductivity whether the measured ac conductivity can be accounted by the tail of the dielectric loss peak which has a distribution of relaxation times. The ac conductivity at different frequencies can be calculated by the following relation:

$$\sigma(\omega) = \frac{\omega \mathcal{E}_0 (\epsilon_0 - \epsilon_\infty) (\omega\tau)^{1-\alpha} \cos(\alpha\pi/2)}{1 + 2(\omega\tau)^{1-\alpha} \sin(\alpha\pi/2) + (\omega\tau)^2 (1-\alpha)}, \quad (8)$$

where \mathcal{E}_0 is the free space permittivity. The calculated values of conductivity $\sigma(\omega)$ from Eq. (8) by using the measured values of ϵ_0 , ϵ_∞ , and f_0 for $\alpha = 0$ and $\alpha = 0.5$ are shown in Fig. 11. The ac conductivity obtained by subtracting the dc conductivity is also shown in Fig. 11. It may be noticed that at frequencies below the relaxation frequency the experimental values fall on the predicted values for $\alpha = 0.5$. The broad distribution of relaxation times corresponding to $\alpha = 0.5$ gives a long tail, and the theoretical conductivity values for $\alpha = 0.5$ are substantially higher than those for $\alpha = 0$ especially above the relaxation frequency. It is clear from Fig. 11 that the measured values of ac conductivity for about three decades above the relaxation frequency can be accounted by the tail of the dielectric loss peak as they agree very well with the theoretical values for $\alpha = 0.5$. However, at higher frequencies the measured values are higher

than the theoretical values. This is quite apparent for the measured value at 3.6 GHz which is two orders of magnitude higher than the theoretical value. Apart from the discrepancy in the room-temperature measured value at 3.6 GHz, the theoretical values of ac conductivity from Eq. (8) predict a slope of 0.5 for $\alpha = 0.5$ at frequencies above the relaxation frequency, while the observed slope at 77 °K is about 0.8. Such a large slope cannot be accounted by the tail of a well-defined loss peak.

The next question arises whether a frequency-dependent conductivity of slope $s = 0.8$ can account for the observed behavior of ac conductivity in the region where measured ac conductivity approaches dc conductivity. At sufficiently low frequencies the ac conductivity is expected to be considerably lower than dc conductivity and the measured ac conductivity should appear frequency independent.¹ Krammers-Kronig relations suggest^{5,6} that the dielectric constant should show a continuous increase with decreasing frequency for a sublinear frequency-dependent ac conductivity. The theoretical values of dielectric constant will become very large and unacceptable for very low frequencies, indicating that the models which predict a sublinear frequency-dependent conductivity are not expected to be valid at sufficiently low frequencies where dc conductivity is substantially higher than ac conductivity and the measured ac conductivity appears frequency independent. However, these models predict a uniform slope at all frequencies, higher than the frequency at which they are expected to break down. This suggests that if the contribution of dc conductivity is removed from the measured ac conductivity in the region where ac conductivity approaches dc conductivity, then the slope should be uniform and have the same value as that at higher frequencies in the region where measured ac conductivity is substantially higher than dc conductivity.¹ However, it is clear from Fig. 11 that the slope of ac conductivity obtained by removing the contribution of dc conductivity in the region where measured ac conductivity approaches dc conductivity is greater than 1 (close to 1.5) below 10^5 Hz and $s \approx 0.5$ for about three decades of frequency above 10^5 Hz, that is, the slope is not uniform in this region. A nonuniform slope is an outcome of the existence of well-defined dielectric loss peaks in the region where measured ac conductivity approaches dc conductivity; such a nonuniform slope is predicted by Eq. (8) and is evident from the calculated values of ac conductivity plotted in Fig. 11.

The above discussions show that the tail of dielectric loss peaks cannot account for the ac conductivity in the region where ac conductivity is substantial higher than dc conductivity, and the

models of sublinear frequency-dependent conductivity cannot account for nonuniform slopes and slopes greater than unity observed at low frequencies in the region where ac conductivity approaches dc conductivity. This suggests that there are two mechanisms responsible for the ac conductivity and the total ac conductivity $\sigma(\omega)$ may be expressed as

$$\begin{aligned} \sigma(\omega) &= \sigma'(\omega) + \sigma''(\omega) \\ &= \int_0^{\infty} \frac{y'(\tau)\omega^2\tau d\tau}{1 + \omega^2\tau^2} + \int_0^{\infty} \frac{y''(\tau)\omega^2\tau d\tau}{1 + \omega^2\tau^2}. \end{aligned} \quad (9)$$

The mechanism responsible for $\sigma'(\omega)$ almost gives a linear dependence of conductivity on frequency, and the distribution function $y'(\tau)$ may be of the form suggested by Pollak which results in ac conductivity of the form given in Eq. (1). The mechanism responsible for $\sigma''(\omega)$ gives a dielectric loss peak with distribution of relaxation time. Assuming a Cole-Cole distribution function for $y''(\tau)$ one can get expression (8) for $\sigma''(\omega)$. The contribution of $\sigma''(\omega)$ dominates for about two to three decades above the relaxation frequency, and the contribution of $\sigma'(\omega)$ becomes dominant only at frequencies which are very much higher than the relaxation frequency and the measured ac conductivity is substantially higher than dc conductivity.

C. Temperature dependence of ac conductivity

It may be noted in Fig. 2 that the conductivity at lower frequencies show a stronger temperature dependence as compared to that at higher frequencies, which causes a decrease in slope s with temperature. If we assume that the slope s of $\sigma(\omega)$ remains unchanged with temperature and any apparent decrease is due to the contribution of $\sigma''(\omega)$, then the temperature dependence of ac conductivity at different frequencies should be explained by taking into account the contributions of $\sigma'(\omega)$ and $\sigma''(\omega)$. In accordance with Eq. (1) $\sigma'(\omega)$ can be expressed as

$$\sigma'(\omega) = BT\omega^s, \quad (10)$$

where parameters B and s are independent of temperatures. The value of these parameters can be calculated from the measured values of conductivity at 95 °K and are given in Table II. The conductivity $\sigma'(\omega)$ at different temperatures and frequencies can then be calculated from Eq. (10). The calculated values are shown by dotted line in Fig. 12. It may be noted that the measured values can be entirely accounted for by the contribution of $\sigma'(\omega)$ up to higher temperatures for higher frequencies. However, above a certain tempera-

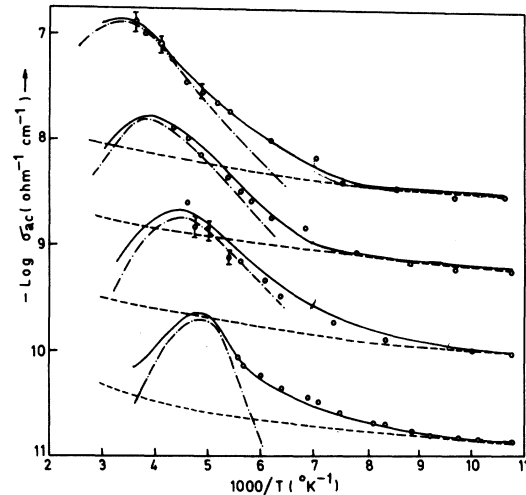


FIG. 12. The circles show the experimental ac conductivity for 67/33 glass at different frequencies and temperature derived by subtracting dc conductivity from the measured conductivity. The chained line shows the contribution of $\sigma'(\omega)$ calculated from Eq. (8). The dotted line gives the contribution $\sigma''(\omega)$ calculated from Eq. (10). The solid line shows the sum of the two calculated values $\sigma'(\omega) + \sigma''(\omega)$.

ture the measured values at different frequencies become substantially higher than the theoretical value of $\sigma'(\omega)$. Probably in this region the contribution of $\sigma''(\omega)$ starts to dominate. The values of $\sigma''(\omega)$ can be calculated from Eq. (8) in the following ways: The static dielectric constant ϵ_0 and the relaxation frequency f_0 at different temperatures can be estimated from Figs. 7 and 10, respectively. The infinite-frequency dielectric constant can be assumed to be independent of temperature and has been taken equal to the intercept in Fig. 7. A temperature-independent^{21,27} value of 0.5 may be assumed for α . Substituting these known values in Eq. (7), the values of $\sigma''(\omega)$ have been computed at different temperatures. For 67% WO_3 -33% P_2O_5 glass these values are shown in Fig. 12 by chained lines. The error in calculated values of $\sigma''(\omega)$, due to the uncertainty in determining the relaxation frequency f_0 , is shown at different temperatures for two frequencies. It may be noted that due to the finite distribution of relaxation times, the uncertainty in the calculated values of $\sigma''(\omega)$ is relatively small near the peak. The large uncertainty in $\sigma''(\omega)$ at temperatures much lower than the temperature at which the peak in $\sigma''(\omega)$ is observed, will not be of any consequence because there the contribution of $\sigma''(\omega)$ becomes much lower than that of $\sigma'(\omega)$. In spite of the uncertainty in the calculated values of $\sigma''(\omega)$, the contribution of $\sigma''(\omega)$ is clearly much higher to the measured conductivity than that of $\sigma'(\omega)$ in the tem-

perature region where strong temperature dependence in measured conductivity is observed.

The sum of the two contributions $\sigma'(\omega)$ and $\sigma''(\omega)$ is shown by solid lines in Fig. 12. The good agreement between the measured values and these calculated by adding the contribution of $\sigma'(\omega)$ and $\sigma''(\omega)$ indicates that the variation of ac conductivity with temperature can be adequately explained by assuming that two mechanisms contribute to the measured ac conductivity.

It may be pointed out that in the present analysis the slope s of $\sigma'(\omega)$ has been assumed to be independent of temperature. However, the small variation of the slope of $\sigma'(\omega)$ with temperature cannot be ruled out in the region where $\sigma''(\omega)$ dominates (Fig. 12) or in any other system in which the mechanism for well-defined dielectric loss peaks does not exist. The strong temperature dependence in ac conductivity and the small slope of the order of 0.5 at high temperatures and low frequencies may entirely be due to $\sigma''(\omega)$ with negligible contribution from $\sigma'(\omega)$.

D. Mechanism of conduction

The optical studies^{36,37} in crystalline transition-metal oxide (TMO) suggests that the valence band may be assumed to be a p band arising from the overlap of p orbitals of the oxygen. The conduction band is assumed to be a d band arising from the d orbitals of the transition-metal ions. The conduction band associated with empty $5d$ states of tungsten is about 4.4 eV above the valence band. The band gap of the pure transition metal oxide corresponds to a good insulator. The much smaller activation energy for conduction in single crystals of these materials suggests the existence of the extrinsic conduction. The obvious donor sites are reduced transition-metal ions created by an oxygen vacancy.

In a normal extrinsic semiconductor once the electrons are excited from lower band to conduction band, they are free to move and for such a conduction mechanism the ac and dc conductivities should be equal. However, the crystalline V_2O_5 ³⁸ and MoO_3 ²⁸ show a frequency-dependent conductivity. The evidence of hopping in the low-temperature phase of WO_3 has been reported.³³ However, the low-temperature ac conductivity of WO_3 has not been reported. Thus in crystalline TMO and TMO glasses, both hopping between the donor states and excitation of the electron from these states to the conduction band are possible. The TM oxides are highly ionic and the hopping conduction has been observed at comparatively much higher temperatures than that in doped Si and Ge. This suggests that localization in the donor states

is strong which may be due to the strong electron lattice interaction giving rise to the polaron formation.^{2,35} The formations of small polarons in tungsten phosphate glasses is indicated by dc conductivity and thermal power studies.³⁹

The optical studies^{36,37} of amorphous WO_3 and MoO_3 films suggest a long band tail which is absent in crystalline films. Band tails^{34,40} have also been observed in V_2O_5 - P_2O_5 glasses. This suggests that there is some change in the energy levels between the amorphous and crystalline transition-metal oxides. Obviously the band edges in amorphous films and glasses may not be as sharp as in single crystals. Crystalline WO_3 is adequately described by a conventional energy-band model,³⁷ and amorphous WO_3 films or amorphous WO_3 - P_2O_5 glasses may be represented by the conventional energy-band model of amorphous semiconductors, with localized band tails and localized states near Fermi level. The two mechanisms of conduction may be associated with the hopping near Fermi level (a linear frequency-dependent conductivity) and hopping of the carriers excited to localized band tails (giving rise to activated dielectric loss peaks). However, Hench⁴¹ has suggested that in the vanadium phosphate glasses the distortion of atomic arrangements in the materials is probably sufficient to satisfy Anderson's criteria thus resulting in complete localization of the energy levels. The energy levels will be localized polarons. Electrical conduction in this case can be considered exclusively as hopping between the polarons states. The possibility of such a mechanism in WO_3 - P_2O_5 glasses cannot be completely ruled out from the present studies, because the origin of two mechanisms of ac conductivity can be visualized in polaron band model as well. The frequency-dependent conductivity may be associated with tunneling and the activated dielectric loss peaks to the hopping over the potential barriers.

CONCLUSIONS

The measured ac conductivity and dielectric constant in tungsten phosphate glasses show that in the region where ac conductivity approaches dc conductivity dielectric loss peaks with a distribution of relaxation times are observed. These loss peaks are confirmed by the dielectric constant measurements.

In the region where ac conductivity is substantially higher than dc conductivity a sublinear dependence of conductivity on frequency is observed which cannot be explained by the tail of dielectric loss peaks. This suggest that two mechanism contribute to the measured ac conductivity.

The strong temperature dependence of ac con-

ductivity starts at higher temperatures for higher frequencies. The temperature dependence of ac conductivity below 10^5 Hz can be explained by expressing the measured ac conductivity $\sigma(\omega)$ as the sum of two conductivities $\sigma'(\omega)$ and $\sigma''(\omega)$ arising from the two different mechanisms. The mechanism giving rise to $\sigma''(\omega)$ is responsible for activated dielectric loss peaks, and may be associated with the hopping of carriers to the localized states in the conduction band tails. $\sigma''(\omega)$ dominates in the region where ac conductivity approaches dc conductivity. The mechanism responsible for $\sigma'(\omega)$ gives a frequency-dependent conductivity of the form $\sigma(\omega) \propto \omega^s$ which is weakly dependent on temperature. The slope s is expected to show lit-

tle or no variation with temperature. The contribution of $\sigma'(\omega)$ to the measured conductivity $\sigma(\omega)$ dominates where $\sigma(\omega)$ is substantially higher than dc conductivity.

ACKNOWLEDGMENTS

The authors are grateful to Professor Mike Sayer, for useful discussions. Thanks are also due to Dr. Prem Swarup, Solid State Physics Laboratory, New Delhi for getting the EPR spectra. Two of us (R.P.T. and J.K.V.) are thankful to the Council of Scientific and Industrial Research, India, for the financial assistance.

*This work forms the part of the thesis submitted by the author to the University of Delhi in 1976 for the award of a Ph.D. degree.

¹N. F. Mott and E. A. Davis, *Electronic Processes in Non-crystalline Materials* (Oxford, Clarendon, 1971).

²I. G. Austin and N. F. Mott, *Adv. Phys.* **18**, 41 (1969).

³M. Pollak, *Philos. Mag.* **23**, 519 (1971).

⁴M. Bottger and V. V. Bryksin, *Phys. Status Solidi B* **9**, 78 (1976).

⁵M. Pollak and T. H. Geballe, *Phys. Rev.* **122**, 1742 (1961).

⁶G. E. Pike, *Phys. Rev. B* **6**, 1571 (1972).

⁷A. K. Jonscher, *J. Non-Cryst. Solids* **8-10**, 293 (1972).

⁸A. E. Owen and J. M. Robertson, *J. Non-Cryst. Solids* **4**, 208 (1970).

⁹M. Kitao, F. Araki, and S. Yamada, *Phys. Status Solidi* **37**, K119 (1976).

¹⁰G. S. Linsley, A. E. Owen, and F. N. Hayatee, *J. Non-Cryst. Solids* **4**, 228 (1970).

¹¹L. I. Lakatos and M. Abkowitz, *Phys. Rev. B* **8**, 1791 (1971).

¹²S. C. Bishop, P. C. Taylor, D. L. Mitchell, and L. H. Sack, *J. Non-Cryst. Solids* **5**, 351 (1971).

¹³M. Sayer, A. Mansingh, A. Reyes, and J. M. Rosenblatte, *J. Appl. Phys.* **42**, 2857 (1971); A. Mansingh, J. Reyes, and M. Sayer, *J. Non-Cryst. Solids* **7**, 12 (1972).

¹⁴M. Pollak, *Phys. Rev.* **138**, 1822 (1965).

¹⁵B. E. Springett, *J. Non-Cryst. Solids* **15**, 179 (1974).

¹⁶S. R. Elliott, *Philos. Mag.* **36**, 1291 (1977); **37**, 533 (1978).

¹⁷I. Thurzo, B. Baranock, and J. Donpovec, *J. Non-Cryst. Solids* **28**, 177 (1978).

¹⁸M. Sayer and A. Mansingh, *Phys. Rev. B* **6**, 4629 (1972).

¹⁹G. F. Lynch, M. Sayer, M. Segel, and G. Rosenblatt, *J. Appl. Phys.* **42**, 2587 (1971).

²⁰M. Sayer and G. F. Lynch, *J. Phys. C* **6**, 3674 (1973).

²¹A. Mansingh, J. K. Vaid, and R. P. Tandon, *J. Phys.*

C **8**, 1023 (1975).

²²A. Mansingh and A. M. Smith, *J. Phys. D* **4**, 560 (1971).

²³A. Mansingh, R. P. Tandon, and J. K. Vaid, *J. Phys. Chem. Solids* **36**, 1267 (1975).

²⁴S. Kabashima, T. Goto, K. Nishimura, and T. Kawakubo, *J. Phys. Soc. Jpn.* **53**, 2757 (1972).

²⁵N. E. Hill, W. E. Vaughan, A. H. Price, and M. Davis, *Dielectric Properties and Molecular Behaviour* (Van Nostrand Reinhold, London, 1969).

²⁶H. E. Taylor, *J. Soc. Glass Technol.* **43**, 124 (1959). R. J. Charles, *J. Appl. Phys.* **32**, 1115 (1961).

²⁷B. S. Rawal and R. K. MacCrone, *J. Non-Cryst. Solids* **28**, 347 (1978).

²⁸M. Sayer, A. Mansingh, J. B. Webb, and J. Woad, *J. Phys. C* **11**, 315 (1978).

²⁹A. Mansingh, M. Sayer, and J. Webb, *J. Non-Cryst. Solids* **28**, 123 (1978).

³⁰Shimakawa Koichi, Nitta Shoji, and Mori Nasaaki, *Phys. Rev. B* **18**, 4348 (1978).

³¹D. L. Kinser, *J. Electrochem. Soc.* **117**, 546 (1970).

³²A. Mansingh, K. N. Srivastava, and B. Singh, *J. Phys. D* **10**, 2117 (1977).

³³J. M. Berak and M. J. Sienko, *J. Solid State Chem.* **2**, 109 (1970).

³⁴I. G. Austin and E. S. Garbett, in *Proceedings of 13th Session of the Scottish Universities Summer School in Physics* (Academic, London, 1975).

³⁵A. J. Bosman and H. J. Van Daal, *Adv. Phys.* **19**, 1 (1970).

³⁶S. K. Deb and J. A. Chopoorian, *J. Appl. Phys.* **37**, 418 (1966).

³⁷S. K. Deb, *Philos. Mag.* **27**, 801 (1973).

³⁸J. Haemers, E. Baetens, and J. Vermik, *Phys. Status Solidi A* **20**, 381 (1973).

³⁹A. Mansingh, A. Dhawan, R. P. Tandon, and J. K. Vaid, *J. Non-Cryst. Solids* **27**, 309 (1978).

⁴⁰C. W. Anderson, *J. Appl. Phys.* **44**, 406 (1973).

⁴¹L. L. Hench, *J. Non-Cryst. Solids* **2**, 250 (1970).